Slow Surface Plasmons in Plasmonic Grating Waveguide

Yun Xu, Jing Zhang, and Guofeng Song

***Abstract*— A metal/air/metal (MAM) plasmonic grating waveguide (PGW) consisting of two parallel silver slabs with periodic corrugations on their inner boundaries is developed to slow down the group velocity of surface plasmon polaritons (SPPs) excited at near-infrared frequencies. For a Gaussian pulse excitation with the full width at half maxim (FWHM) of 222fs and the center wavelength of 1.58μm, the group velocity of 0.034c and the group velocity dispersion (GVD) of 0.8ps/mm/nm can be achieved in finite-difference time-domain (FDTD) simulations with pulse excitation. Furthermore, a chirped PGW with varying groove depth is also demonstrated as a way to trap light by adopting continuous excitation.**

***Index Terms*— Plasmonic grating waveguide (PGW), slow wave, surface plasmon polaritons (SPPs).**

I. Introduction

THE VELOCITY of light in vacuum is extremely fast ($c \cong 3 \times 10^8 m/s$). This ultrafast speed is advantageous for efficient data transmission, but difficult for control of the optical signal in time domain. Slow light is a technology now being investigated as a solution to overcome this problem. Well knowingly, it had been demonstrated that exotic material dispersion in ultra-cold atoms driven by a laser can dramatically reduce the light velocity to 17m/s [1]. This achievement was amazing, but "slow light on a chip" at room temperature remains a great challenge. It is anticipated to bring in a wealth of photonic applications, especially in the fields of telecommunications and optical data processing [2]. "Slow light on a chip" can be realized by artificial resonance created by structured materials, such as Photonic Crystal Waveguides [3]–[6] (PCW) and Plasmonic Bragg Grating [7]–[13] (PBG). Moreover, slow light can also be realized in multi-nanoresonator-coupled waveguide systems [14]. Surface Plasmon Polaritons [15] (SPPs) assisted metallic structure has attracted much attention recently because of its potential for spatial confinement of electromagnetic (EM) energy within the sub-wavelength dimension over broad bandwidth [16] and it gives the possibility of plasmonics to break the diffraction limit [17]. Therefore SPPs become suitable candidates for light guiding in photonic circuits. Although ohmic heating losses can never be completely eliminated in plasmonic circuitry, recent progress allowing for SPPs propagation lengths in the range of millimeters enable a high density of multifunctional plasmonic components to be integrated [18,19]. Thus the precise control of the SPPs in the sub-wavelength volume will play a vital role in all-optical circuitry. SPPs are charge density waves on the surface of materials with free electrons (metals, plasmas, etc.) propagating along the interface between a conductor and a dielectric medium of permittivities ε_{p} and ε. SPPs exist only for TM polarization, and the dispersion relation is $k = (\omega/c)\sqrt{\varepsilon\varepsilon_p(\omega)/[\varepsilon + \varepsilon_p(\omega)]}$. The group velocity of the propagating SPPs is usually determined by the material's refractive index, which cannot be varied very much, but it can be drastically altered by the photonic band structure engineering [20]. Thus it is possible to obtain an ultra-small group velocity by tuning the metallic structure to build a very flat dispersion relation [21].

The previous investigations about slow light in plasmonic nanostructures [22]–[26] are mainly focus on the group velocity derived from the photonic band analyses. In this letter we obtain the group velocity of SPPs by employing a Gaussian pulse excitation in the Finite-difference time-domain (FDTD) simulation, which provides direct evidence for the slow light process.

II. Slow Light Property of the Proposed Plasmonic Waveguide

Our proposed nanoscale system consists of two parallel silver slabs with periodic corrugations on their inner boundaries, as shown in the inset of Fig. 1(a), where w is the width of the grooves, h is the depth, g is the gap and p is the period of the grating. In order to calculate the precise dispersion relation, a 2-D FDTD simulation on one unit cell of this PGW is employed. The Perfectly Matched Layer (PML) absorbing boundary condition is used in the z direction, and the Bloch boundary condition in the x direction. We excite eigenmodes by a point source and compute the frequency spectrum of the time-domain response, where each peak in the spectrum corresponds to an eigen frequency. The dispersion relation of the SPPs can therefore be obtained by finding the values of eigen frequency ω and the corresponding wave vector kx. We employ the Drude-Lorentz model to evaluate the dielectric constant of silver by fitting the experimental data [27]. The fitting model is described as [28]

Manuscript received August 21, 2012; revised December 9, 2012; accepted January 3, 2013. Date of current version February 4, 2013. This work was supported in part by the National Basic Research Program of China (973 Program) under Grant 2011CBA00608 and Grant 2012CB619203, in part by the National Natural Science Foundation of China under Grant 61177070, Grant 60906027, Grant 60906028, and Grant 61036010, in part by the Beijing Natural Science Foundation of China under Grant 4112058, and in part by the National Key Research Program of China under Grant 2011ZX01015-001.

The authors are with the Institute of Semiconductors, Chinese Academy of Science, Beijing 100083, China (e-mail: xuyun@semi.ac.cn; gcrrr@semi.ac.cn; sgf@semi.ac.cn).

Color versions of one or more of the figures in this letter are available online at http://ieeexplore.ieee.org.

Digital Object Identifier 10.1109/LPT.2013.2238667

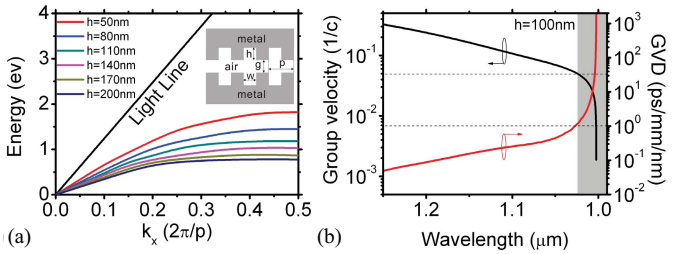

Fig. 1. (a) Dispersion relations calculated for w = 50 nm, and p = 100 nm and six different groove depths (h = 50 nm, 80 nm, 110 nm, 140 nm, 170 nm, and 200 nm). Inset: schematic of PGW. Group velocity and GVD for (b) h = 100 nm as a function of wavelength. Gray areas indicate the GVD is larger than 1ps/mm/nm.

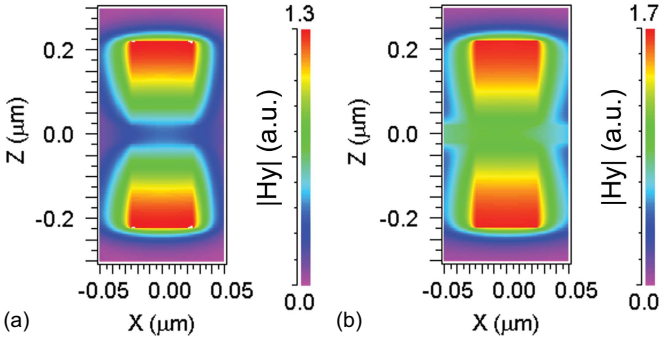

Fig. 2. Field distributions of |Hy| in one unit cell for the continuous excitation at (a) 1.58 μm and (b) 2 μm, respectively.

TABLE I

PARAMETERS FOR THE DRUDE-LORENTZ MODEL

j	ω_j(rad/μm)	a_j	γ_j
1	4.1326	7.9247	19.6807
2	22.6941	0.5013	2.2892
3	41.4531	0.0133	0.3292
4	46.001	0.8266	4.6391
5	102.759	1.1133	12.25
ω_p = 41.946rad/μm, $1/\tau$=0.2431rad/μm			

$$\varepsilon(\omega) = 1 - \frac{\omega_p^2}{\omega^2 + i\omega/\tau} + \sum_{j=1}^{5} \frac{a_j \omega_j^2}{(\omega_j^2 - \omega^2) - i\omega\gamma_j} \quad (1)$$

Where ωp is the plasma frequency, $1/\tau$ is the relaxation rate, ω_j is the resonant frequency, γ_j is the spectral width of the Lorentz oscillation, and a_j is weighting factor. The values of these parameters are listed in table I.

After the band calculations for various parameters, it is found that the dispersion curve is very sensitive to the change of the depth h. The calculated dispersion curves of SPPs in the first Brillouin zone for the PGW with w = 50 nm, p = 100 nm, g = 40 nm and six different depths (h = 50 nm-200 nm) are demonstrated in Fig. 1(a). Noticeably, the group velocity of the SPPs ($V_g = d\omega/dk$) decreases significantly, when the wave vector k asymptotes π/p (the Brillouin boundary). From the dependence of the dispersion curve on the depth, it is observed that the increase of the depth leads to the shift of the cutoff frequency to low frequency. The depth-dependent dispersion of plasmonic surface grating has been reported by the pervious experimental work[10]. Furthermore, the dispersion curve becomes flat with the depth varying from 50 nm to 200 nm, which implies that a lower group velocity requires a deeper groove. The group refractive index is defined as

$$n_g = \frac{c}{V_g} = c\frac{dk_x}{d\omega} = \frac{d(n\omega)}{d\omega} = n + \omega\frac{dn}{d\omega}. \quad (2)$$

where c is the light velocity in vacuum and V_g is the group velocity of the SPPs.

The GVD is defined as

$$D = \frac{dv_g^{-1}}{d\lambda} = \frac{1}{c}\frac{dn_g}{d\lambda}. \quad (3)$$

By using the Eqs. (2) and (3), the group velocities and group velocity dispersions at different wavelengths can be obtained, as shown in Fig. 1(b). The group velocity of c/600 can be achieved for the depth of 100 nm. Although the lowv_g can be obtained near the cutoff frequencies, it is difficult the simultaneously achieve a small GVD without special design [29]. For GVD less than 1ps/mm/nm, the group velocity can just reach about 0.05c for h = 100 nm at around 1μm as illustrated by the dash lines in Fig. 1(b). In order to understand the origin of the slowdown effects, it is instructive to investigate the field distributions in the PGW. Fig. 2 show the distributions of field components |Hy| for h = 200 nm at 1.58μm and 2μm, which corresponds to the group velocities of c/30 and c/8 respectively. In the uniform metal/insulator/metal (MIM) plasmonic gap waveguide, two TM plasmon modes [30] (plasmon modes are all TM) exist: symmetric (TM_0-like) with no cutoff gap and antisymmetric (TM_1-like) with a cutoff gap below ~λ/2n (n is the refraction index of the dielectric core). Oscillating modes exist as well as in the normal waveguide, and each has a cutoff gap below which it becomes evanescent with a very high decay rate. Since the gap of air core in our proposed system is less than 50 nm, only the symmetric TM plasmon mode can be observed in the PGW. From the field distributions in Fig. 2(a), the SPP resonances can be obviously observed inside the grooves for 1.58μm. Each unit cell performs like an isolate cavity and the coupling between the neighborhood unit cells is very weak, as shown in Fig. 2(a). It is the weakly coupled resonance that makes the dispersion curves rather flat [31]. On the contrast, the round trip phase change in the groove cannot satisfy the resonance condition for 2μm. From Fig. 2(b), the strong coupling between the neighborhood unit cells is observed. The energy has been transferred from one unit to another obviously. Consequently, the intrinsic differences between the two situations are that the SPPs are coupled into the grooves and form the cavity resonant mode [32],[33] along the z direction at 1.58μm while the SPPs are concentrated in the gaps and maintain the plasmon waveguide mode along the x direction at 2μm. The working band of our structure can be predicted by searching the resonant frequency in the unit cell [34]. By using this property, we can change the parameters to make the slow light system work in any desired frequency.

Subsequently we choose the structure with w = 50 nm, p = 100 nm, g = 40 nm and h = 200 nm as the

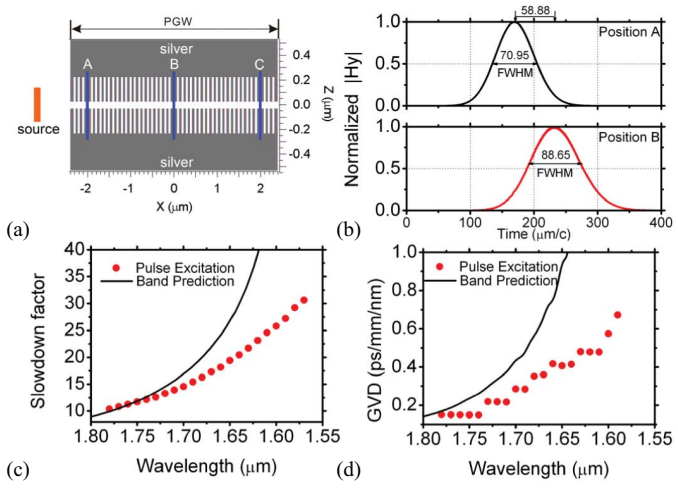

Fig. 3. (a) Schematic of FDTD simulation system. (b) Pulse profiles recorded by the detector at position A (upper) and B (bottom) for the pulse with center wavelength of 1.58 μm. (c)–(d) Slow down factor and GVD as a function of wavelength. Band prediction and pulse excitation denote the results derived from the dispersion curve and the simulations with pulse excitation respectively.

target to investigate the group velocity of the SPPs near the telecom wavelength of 1.55μm. To validate the slow-down effects of the propagating SPPs, a Gaussian profile pulse (TM-polarization) with the Full Width at Half Maxim (FWHM) of 66.6μm/c (222fs) is launched in the 2-D FDTD simulation (The grid size is $\Delta x = 2$ nm, $\Delta z = 5$ nm, $\Delta t = 10$ nm, the area of the simulation region is 8μm 1μm), and the magnetic field component (Hy) is monitored at three positions with 2μm interval (A (-2μm), B (0μm), and C (2μm)), as shown in Fig. 3(a). The total length of the PGW consisting of 48 unit cells is 4.8μm. Therefore, the profiles of the propagating pulse can be recorded at different positions in the time domain. The slowdown factor can be obtained by measuring the time of the pulse propagating from the position A to B or C. Fig. 3(b) demonstrates the pulse profiles recoded at position A and B for the excitation pulse with the center wavelength of 1.58μm. The delay time of 58.88μm/c is obtained after the propagation length of 2μm. Thus, the group velocity of 0.034c and the slowdown factor of 29.44 are achieved. Due to the large GVD, the pulse width is obviously broadened from 70.95μm/c to 88.96μm/c. This serious distortion will reduce the delay-bandwidth product (DBP) [35] in optical communications, which means there is a certain competition between the delay time and the bandwidth. Additionally, air is adopted as dielectric material in the gap between the two metallic gratings, so the slowdown factor is equivalent to the group refractive index n_g. We depict the slowdown factor and the GVD as the function of wavelength in Fig. 3(c)–(d), where the black solid lines indicate the results derived from the dispersion curves and the red dots represent the results obtained from the simulations with 222fs pulse excitation. Since the bandwidth of the pulse is about 25 THz, the slowdown factor in the simulations with pulse excitation is lower than that predicted by the dispersion curve, so does the GVD. For the 222fs pulse, the slowdown factor of 30

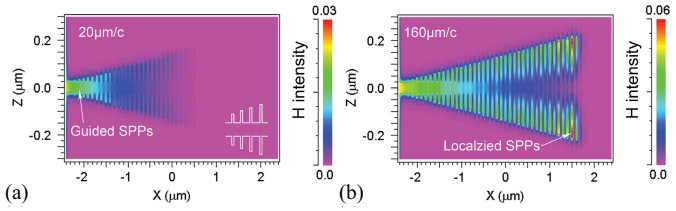

Fig. 4. Distributions of H field intensity in the chirped PGW for the continuous excitation after the simulation times of (a) 20 μm/c and (b) 160 μm/c. In the proposed structure, p is fixed at 100 nm and hincreases from 0 nm to 240 nm over waveguide length of 48 periods.

accompanied with the GVD of 0.8ps/mm/nm can be achieved at about 1.58μm. When the wavelength of incident light is longer than 1.8μm, the slowdown factor varies slowly below 8 and the GVD stays at around 0.1ps/mm/nm.

Fig. 1(a) also gives us a clue on how the SPPs can be concentrated and trapped. A chirped PGW structure is considered, where the depth h gradually increases uniformly along the propagation direction, as illustrated in the inset of Fig. 4(a). If the excitation frequency is fixed, it is expected that the group velocity of the SPPs will be gradually reduced along the propagation direction and can even approach almost zero at the cutoff location, where the local cutoff frequency is the same as the frequency of the incident light. The SPPs-trapping property of the chirped structure with p = 100 nm and h increasing from 0 nm to 240 nm over waveguide length of 48 periods can be validated by using FDTD simulations. Fig. 4(a)–(b) show the H field intensity distributions of light simulated against the continuous-wave excitation at 1.55μm after simulation times of 20μm/c and 160μm/c. It is clearly seen that the light is coupled into the guided SPPs in the separation of chirped PGW and the SPPs penetrates into the grooves step by step along the propagation direction. The red spots in Fig. 4(b) indicate the localized SPPs in the 40th groove. This localization does not mean the complete stop of optical energy at the point. Once the resonance is formed, the increase in accumulated optical energy is saturated and reflection starts. It takes about 140μm/c to couple the SPPs from the input port to the 40th groove, which implies an average group velocity of about 0.028c. In addition, SPPs at different excitation frequencies will be trapped at different grooves, known as "rainbow trapping" [36],[37]. Thus our proposed PGW structure can be integrated on a chip to realize an automatic optical demodulator in the sub-wavelength scale.

Moreover, the problem of coupling light into the proposed MIM structure is not addressed in this letter. The nano-sized gap leads to a low coupling efficiency, but a tapered plasmon gap waveguide [7] can be employed as an input port, which exhibits high efficiently plasmon-assisted coupling (about 70%) from a micrometer size silica-air-clad dielectric waveguide to a 50 nm plasmon waveguide [38],[37]. The gap is filled with air which can also be substituted by the gain media to compensate the absorption loss [39].

III. Conclusion

In conclusions, we construct a slow light system consisting of two parallel silver slabs with periodic corrugations on their

inner boundaries, which exhibit rather flat dispersion relation near the Brillouin boundary. A Gaussian pulse is employed to validate the slow light characteristic of our proposed structure in FDTD simulations. The group velocity of 0.034c and the GVD of 0.8ps/mm/nm are achieved for the 222fs pulse with the center wavelength of 1.58μm. By observing the field distribution in one unit cell of the PGW, we find that the slowdown effects originate from the forming of the SPP resonant modes inside the grooves. A chirped PGW with varying groove depth along the propagation direction is demonstrated to trap light and an average group velocity of 0.028c is obtained in the simulation with the continuous excitation. Since the propagation properties of the SPPs can be controlled by the surface geometry, our proposed structure can be fabricated on a chip to realize optical signal processing applications in photonic circuits.

REFERENCES

[1] L. V. Hau, S. E. Harris, Z. Dutton, and C. H. Behroozi, "Light speed reduction to 17 metres per second in an ultracold atomic gas," *Nature* vol. 397, no. 6720, pp. 594–598, 1999.

[2] T. F. Krauss, "Why do we need slow light?" *Nature Photon.*, vol. 2, no. 8, pp. 448–450, 2008.

[3] T. BaBa, "Slow light in photonic crystals," *Nature Photon.*, vol. 2, no. 8, pp. 465–473, 2008.

[4] M. Notomi, K. Yamada, A. Shinya, J. Takahashi, C. Takahashi, and I. Yokohama, "Extremely large group-velocity dispersion of line-defect waveguides in photonic crystal slabs," *Phys. Rev. Lett.*, vol. 87, no. 25, p. 253902 2001.

[5] D. Mori and T. Baba, "Dispersion-controlled optical group delay device by chirped photonic crystal waveguides," *Appl. Phys. Lett.*, vol. 85, pp. 1101–1103, Jun. 2004.

[6] Y. A. Vlasov, M. O. Boyle, H. F. Hamann, and S. J. McNab, "Active control of slow light on a chip with photonic crystal waveguides," *Nature*, vol. 438, pp. 65–69, Sep. 2005.

[7] J. Zhang, L. Cai, W. Bai, Y. Xu, and G. Song, "Slow light at terahertz frequencies in surface plasmon polariton assisted grating waveguide," *J. Appl. Phys.*, vol. 106, no. 10, pp. 103715-1–103715-3, 2009.

[8] Y. Gong, L. Wang, X. Hu, X. Li, and X. Liu, "Broad-bandgap and low-sidelobe surface plasmon polariton reflector with Bragg-grating-based MIM waveguide," *Opt. Express*, vol. 17, no. 16, pp. 13727–13736, 2009.

[9] Y. Qi, D. Gan, J. Ma, J. Cui, C. Wang, and X. Luo, "Spectrally selective splitters with metal-dielectric-metal surface plasmon waveguides," *Appl. Phys. B*, vol. 95, no. 4, pp. 807–812, 2009.

[10] S. Balci, A. Kocabas, C. Kocabas, and A. Aydinli, "Induced absorption dynamics in quantum dot based waveguide electroabsorbers," *Appl. Phys. Lett.*, vol. 97, no. 12, pp. 121103-1–121103-3, 2010.

[11] C. Li, X. Zhang, Y. Song, D. Kong, and Y. Wang, "Precise control of group velocity by pulsewidth in a plasmonic superlattice," *IEEE Photon. Technol. Lett.*, vol. 23, no. 17, pp. 1243–1245, Sep. 1, 2011.

[12] G. Kumar, S. Pandey, A. Cui, and A. Nahata, "Planar plasmonic terahertz waveguides based on periodically corrugated metal films," *New J. Phys.*, vol. 13, pp. 033024-1–033024-13, Mar. 2011.

[13] G. Wang, H. Lu, and X. Liu, "Trapping of surface plasmon waves in graded grating waveguide system," *Appl. Phys. Lett.*, vol. 101, no. 1, pp. 013111-1–013111-3, 2012.

[14] H. Lu, X. Liu, and D. Mao, "Plasmonic analog of electromagnetically induced transparency in multi-nanoresonator-coupled waveguide systems," *Phys. Rev. A*, vol. 85, no. 5, pp. 053803-1–053803-7, 2012.

[15] H. Raether, *Surface Plasmons*. New York: Springer-Verlag, 1988.

[16] W. L. Barnes, A. Dereux, and T. W. Ebbesen, "Surface plasmon subwavelength optics," *Nature*, vol. 424, p. 824–830, Aug. 2003.

[17] S. Jetté-Charbonneau, R. Charbonneau, N. Lahoud, G. Mattiussi, and P. Berini, "Demonstration of Bragg gratings based on long ranging surface plasmon polariton waveguides," *Opt. Express*, vol. 13, no. 12, pp. 4674–4682, 2005.

[18] M. Sandtke and L. Kuipers, "Slow guided surface plasmons at telecom frequencies," *Nat. Photon.*, vol. 1, pp. 573–576, Sep. 2007.

[19] E. Ozbay, "Plasmonics: Merging photonics and electronics at nanoscale dimensions," *Science*, vol. 311, no. 5758, pp. 189–193, 2006.

[20] J. B. Pendry, L. Martin-Moreno, and F. J. Garcia-Vidal, "Mimicking surface plasmons with structured surfaces," *Science*, vol. 305, no. 5685, pp. 847–848, 2004.

[21] F. J. Garcia-Vidal, L. Martin-Moreno, and J. B. Pendry, "Surfaces with holes in them: New plasmonic metamaterials," *J. Opt. A, Pure Appl. Opt.*, vol. 7, no. 2, p. S97, 2005.

[22] Q. Gan, Z. Fu, Y. J. Ding, and F. J. Bartoli, "Ultrawide-bandwidth slow-light system based on THz plasmonic graded metallic grating struct ures," *Phys. Rev. Lett.*, vol. 100, no. 25, pp. 256803-1-256803-4, 2008.

[23] Q. Gan, Y. J. Ding, and F. J. Bartoli, "'Rainbow' trapping and releasing at telecommunication wavelengths," *Phys. Rev. Lett.*, vol. 102, no. 5, pp. 056801-1–056801-4, 2009.

[24] A. Kocabas, S. S. Senlik, and A. Aydinli, "Slowing down surface plasmons on a Moiré surface," *Phys. Rev. Lett.*, vol. 102, no. 6, pp. 063901-1-063901-4, 2009.

[25] A. Karalis, E. Lidorikis, M. Ibanescu, J. D. Joannopoulos, and M. Soljacic, "Surface-plasmon-assisted guiding of broadband slow and subwavelength light in air," *Phys. Rev. Lett.*, vol. 95, no. 6, pp. 063901-1–063901-4, 2005.

[26] A. Karalis, J. D. Joannopoulos, and M. Soljacic, "Plasmonic-dielectric systems for high-order dispersionless slow or stopped subwavelength light," *Phys. Rev. Lett.*, vol. 103, no. 4, p. 043906, 2009.

[27] *Handbook of Optical Constants of Solids*, E. D. Palik, Ed., Academic, New York, 1985.

[28] A. Tip, "Linear dispersive dielectrics as limits of Drude-Lorentz systems," *Phys. Rev. E*, vol. 69, pp. 016610-1–016610-5, Jan. 2004.

[29] G. Wang, H. Lu, and X. Liu, "Dispersionless slow light in MIM waveguide based on a plasmonic analogue of electromagnetically induced transparency," *Opt. Express*, vol. 20, no. 19, pp. 20902-1–20902–7, 2012.

[30] E. Feigenbaum and M. Orenstein, "Modeling of complementary (Void) plasmon waveguiding," *J. Lightw. Technol.*, vol. 25, no. 9, pp. 2547–2562, Sep. 1, 2007.

[31] V. Kuzmiak, A. A. Maradudin, and A. R. McGurn, "Photonic band structures of two-dimensional systems fabricated from rods of a cubic polar crystal," *Phys. Rev. B*, vol. 55, no. 7, pp. 4298–4311, 1997.

[32] B. Wang, Y. Jin, and S. He, "Design of subwavelength corrugated metal waveguides for slow waves at terahertz frequencies," *Appl. Opt.*, vol. 47, no. 21, pp. 3694–3700, 2008.

[33] T. F. Krauss, "Slow light in photonic crystal waveguides," *J. Phys. D, Appl. Phys.*, vol. 40, no. 9, pp. 2666–2670, 2007.

[34] W. C. Tan, T. W. Preist, J. R. Sambles, and N. P. Wanstall, *Phys. Rev. B*, vol. 59, no. 19, pp. 12661–12666, 1999.

[35] D. Mori and T. Baba, "State-of-the-art photonic nanostructure devices," *Opt. Express*, vol. 13, no. 23, pp. 9398–9408, 2005.

[36] K. L. Tsakmakidis, A. D. Boardman, and O. Hess, "'Trapped rainbow' storage of light in metamaterials," *Nature*, vol. 450, pp. 397–401, Nov. 2007.

[37] J. Zhang, L. Cai, W. Bai, and G. Song, "Flat surface plasmon polariton bands in Bragg grating waveguide for slow light," *J. Lightw. Technol.*, vol. 28, no. 14, pp. 2030–2036, Jul. 15, 2010.

[38] P. Ginzburg, D. Arbel, and M. Orenstein, "Guiding of a one-dimensional optical beam with nanometer diameter," *Opt. Lett.*, vol. 31, pp. 3288–3290, Jun. 2006.

[39] J. A. Dionne, E. Verhagen, A. Polman, and H. A. Atwater, "Are negative index materials achievable with surface plasmon waveguides? A case study of three plasmonic geometries," *Opt. Express*, vol. 16, no. 23, pp. 19001–19017, 2008.